Blockchain-Based Stochastic Energy Management of Interconnected Microgrids Considering Incentive Price

Morteza Dabbaghjamanesh, *Senior Member, IEEE*, Boyu Wang, *Member, IEEE*, Abdollah Kavousi-Fard, *Senior Member, IEEE*, Nikos D. Hatziargyriou, *Life Fellow, IEEE*, and Jie Zhang, *Senior Member, IEEE*

***Abstract*—Decomposing the large distribution grids into interconnected microgrids (MGs) can potentially enhance the power system's efficiency, sustainability, resiliency, and reliability. However, energy management within the entire network would be more complicated and challenging. This article develops a novel energy management framework for interconnected MGs based on a blockchain technology. Utilizing the blockchain technology can potentially enhance the system security, and also reduce the system risks, mitigate financial fraud, and cut down the operational cost. A priority list is first defined to get into an efficient energy tradeoff within the interconnected MGs. Moreover, the incentive contract is proposed to provide a price discount for a party that purchases more power from one sub-MG. A stochastic framework based on the unscented transform technique is also established to manage the uncertainties associated with hourly load demands and output power of renewable energy sources. The proposed model is formulated as a mixed-integer linear programming problem and solved through the blockchain-based energy/power management algorithm. The case study includes residential, industrial, and commercial MGs—namely, three residential, one commercial, and one critical load (hospital). The simulation results show the high efficiency and effectiveness of the proposed model and validate its economic and reliability merits.**

***Index Terms*—Blockchain, interconnected microgrids (MGs), power grid security, priority list, uncertainty.**

Manuscript received September 1, 2020; revised December 27, 2020; accepted January 13, 2021. Date of publication February 16, 2021; date of current version September 17, 2021. Recommended by Associate Editor L. Xie. *(Corresponding author: Morteza Dabbaghjamanesh.)*

Morteza Dabbaghjamanesh and Jie Zhang are with the Department of Mechanical Engineering, and also with the Department of Electrical and Computer Engineering (Affiliated), The University of Texas at Dallas, Richardson, TX 75080 USA (e-mail: mortezadabba@utdallas.edu; jiezhang@utdallas.edu).

Boyu Wang is with Tacoma Public Utilities, Tacoma, WA 98409 USA (e-mail: bwang1@cityoftacoma.org).

Abdollah Kavousi-Fard is with the Department of Electrical and Electronics Engineering, Shiraz University of Technology, Shiraz 71557, Iran (e-mail: kavousi@sutech.ac.ir).

Nikos D. Hatziargyriou is with the National Technical University of Athens, 15773 Athens, Greece (e-mail: nh@power.ece.ntua.gr).

Digital Object Identifier 10.1109/TCNS.2021.3059851

Nomenclature

Sets/Indices

Ω^D/d	Set/index of load.
$\Omega^B/l,n$	Set/index of distribution nodes in microgrid *m*.
Ω^{DL}	Set of distribution lines.
Ω^{DG}/i	Set/index of DGs.
Ω^{MG}/m	Set/index of MGs.
Ω^{ES}/e	Set/index of energy storage.
Ω^T/t	Set/index of time periods.
$\underline{(.)}, \overline{(.)}$	Maximum, minimum values for a variable.

Parameters

C_{im}	Generation cost of DG *i* in microgrid *m*.
D_{dmt}	Demand of load *d* in microgrid *m* at time *t*.
R^U_{im}, R^D_{im}	Ramp up/down rate for DG *i* in microgrid *m*.
R, X, Z	Resistance, reactance, and impedance of distribution lines.
S^U_{im}, S^D_{im}	Startup/shutdown cost of DG *i* in microgrid *m*.
$\chi^{on}_{im}, \chi^{off}_{im}$	Number of successive ON/OFF hours for DG unit *i* in microgrid *m*.
χ^c_{em}, χ^d_{em}	Number of successive charging/discharging hours for energy storage *e* in microgrid *m*.
λ^P_m, λ^S_m	Purchase/selling power cost of microgrid *m*.
τ^U_{im}, τ^D_{im}	Minimum up/down time of DG *i* in microgrid *m*.
$\tau^c_{emt}, \tau^d_{emt}$	Minimum charging/discharging time for energy storage *e* in microgrid *m* at time *t*.

Variables

I^L	Current flow of distribution lines.
P^P_{mt}, P^S_{mt}	Purchase/selling power in microgrid *m* at time *t*.
P_{imt}	Active power generated by DG *i* in microgrid *m* at time *t*.
P^{ES}_{emt}	Output power of energy storage *e* in microgrid *m* at time *t*.
P^c_{emt}, P^d_{emt}	Charging/discharging power of the energy storage *e* in microgrid *m* at time *t*.
P^L/Q^L	Active/reactive power flow of distribution lines.
V	Buses voltage magnitude.
W	Weight factor.
w^L	Status of the distribution line.
ΔV	Distribution lines variable that is needed to apply KVL.
$\vartheta_{emt}, \rho_{emt}$	Charging/discharging status of energy storage *e* in microgrid *m* at time *t* (binary variable).
μ	Mean value.
σ	Covariance.
δ_{imt}	Status of DG *i* in microgrid *m* at time *t* : 1 if DG is on, and 0 otherwise.
$\delta^P_{mt}/\delta^S_{mt}$	Purchasing/selling binary status of microgrid *m* at time.
ψ_{emt}	State of charge (SOC) for energy storage *e* in microgrid *m* at time *t*.

I. Introduction

MICROGRIDS (MGs) are small distribution grids that are comprised of distributed energy resources (DERs) and loads, which can operate in both grid-connected and islanded modes [1]. This ability can lead to significant advantages, such as higher resiliency, higher reliability, lower losses, and lower operational costs. MGs are considered as the most effective way to exploit the full benefits of DER if coordinated properly by the distribution system operator (DSO) [2]. However, effective and reliable energy management is required, considering the uncertainty associated with renewable energy power and load demands.

Depending on the ownership and operating model of the MGs, they may have different objectives and policies from the DSO, who is responsible for the security and power flow management within the wider distribution network. Since the network is physically interconnected, any change in any subsystem (MGs) can have an impact on other subnetworks. According to the IEEE standard 1574.4, the operation, security, and reliability of the power grids can be improved by decomposing the large grids into interconnected MGs [3]. However, the energy management of the interconnected MGs would be more complicated and challenging.

Efficient energy management of a single MG has been investigated extensively in the literature [4]–[9]. For instance, in [4] a robust optimization approach was developed, considering load and distributed generator (DG) uncertainties. The optimal energy management of multiperiod islanded MG was investigated in [5], where the author utilized the Bender decomposition technique for grid-connected and islanded modes to overcome the complexity of the problem. The economic dispatch problem within a single MG was studied in [6]–[8], where the authors considered additional spinning reserve to guarantee the stability of MG operation. In [9], the market perspective of MG was studied by employing mixed-integer linear programming (MILP). The high penetration of renewable energy sources was investigated in [10] and [11] by considering energy storage to manage uncertainties. The optimal operation of an MG, considering dynamic line rating (DLR) limitations of distribution lines, was investigated in [12].

Although energy management of a single MG has been widely researched, the impact of interconnectivity within a system of several interconnected MGs has not been well investigated. The energy management of interconnected MGs based on multiagents was studied in [13], where the main objective was to minimize the power mismatch. An effective energy management of interconnected MGs was investigated in [14], where the authors considered the uncertainties of load demand in some of the MGs together with constant loads. Reference [15] solved the energy management of several MGs through a bilevel formulation, where the upper level solved the central market clearing problem and the power dispatch was solved in the lower level problem. The economic dispatch of interconnected MGs with uncertainties (in generation and demand) was studied in [16], whereas [17] developed a robust optimization technique for renewable-based interconnected MGs. In [18], a decentralized framework based on a bilevel optimization was proposed, where the upper level dealt with the negotiations among all entities and the lower level changed the nonconverging penalties to make the problem feasible. The authors utilized Monte Carlo simulations (MCs) to model the associated uncertainties.

The energy management of interconnected MGs has been investigated in the above work. However, a decentralized, transparent, and secure trade of energy among the interconnected MGs has not been well investigated in the literature. To this end, this article proposes to use the blockchain technique in energy trading. A blockchain is a decentralized, transparent, and secure technique, which includes a public ledger of all cryptocurrency transactions to be accessible by all subsystems [19]. The most recent transactions are continuously recorded and added to the blockchain in a chronological order. This allows market participants to keep track of digital currency transactions without central record keeping. Each node gets a copy of the blockchain, which is updated automatically. It has been reported in the literature that the blockchain decentralized framework

offers significant advantages, such as higher transparency, security, traceability, efficiency, speed, and low cost [20]–[22]. Hence, in this article, a new framework for interconnected MGs is developed by implementing blockchain based on an incentive contract. The proposed incentive contract technique provides an option for one MG to get more discount when purchasing more power. To have a fair and effective energy management strategy, a priority list is defined based on the common and critical loads. It should be noted that in traditional power grids, the authority is given to DSO to manage distribution feeders. However, in modern power systems, the DSO and MG may have different utility operators. Therefore, power/energy management in different MGs may be based on different rules and policies. On the other hand, since the entire grid is composed of interconnected MGs, any change in any of the subsystems will affect the network operation from the system-level perspective, due to the high level of interconnectivity within the system. Due to these reasons, a full blockchain algorithm is essential to enhance not only the security of an MG, but also to reduce system risks, mitigate financial fraud, increase the surety of power trading, and cut down the operational cost of the entire network. Considering all these factors, as well as incentive prices for active agents within the network, the blockchain-based energy management will become a complicated and challenging problem to solve.

Furthermore, a stochastic framework based on the unscented transform (UT) technique [23]–[24] is employed to manage the uncertainties in the power output of DERs and load demands. The UT method is an estimation technique, which has shown significant advantages compared to other alternatives, e.g., MC simulations that need a considerable number of iterations to converge and it is not suitable for correlated environments [25]. The main contribution of this article can be summarized as follows.

1) A new fully decentralized, transparent, and secure framework based on blockchain is developed for energy management of interconnected MGs. The proposed framework includes decentralized processing with the minimal exchange of power among interconnected MGs.
2) A priority list is developed based on incentive contracts and various types of loads, including residential, industrial, and commercial loads.
3) A nonlinear stochastic framework is developed to model the uncertainties associated with the problem based on the UT technique.

The rest of the article is organized as follows. Section II describes the mathematical modeling of the proposed problem. Section III presents the stochastic framework based on the UT technique. Section IV describes the blockchain technology, as well as the incentive price. Section V summarizes the solution procedure of the proposed problem. Section VI shows the simulation results, followed by the conclusion in Section VII.

II. Effective Scheduling of Interconnected MGs

In this section, a thorough mathematical model is developed for the power management of interconnected MGs. A single objective optimization problem is formulated, seeking to minimize the total operation cost of the interconnected MGs while satisfying all the associated constraints. Fig. 1 shows the schematic framework of the proposed interconnected MGs network that includes a hospital MG (as crucial load), a commercial MG (as intermediate level load), and residential MGs (as noncrucial loads). The individual MGs manage their own power generation/consumption to the extent that power balance is satisfied in the MG. Once there is power surplus or deficit in individual MGs, the blockchain technology will control and implement power management among MGs and allow individual MGs to share certain generation/consumption. It should be noted that the residential MGs are separated and considered as the nonurgent loads. The proposed problem is formulated as an MILP problem, which has a fast convergence speed, as well as providing a general framework for modeling a large variety of problems. Also, the MILP problem can be solved by a standard mathematical programming solver, and CPLEX is adopted in this article. The objective function and the constraints are explicitly described in the following sections.

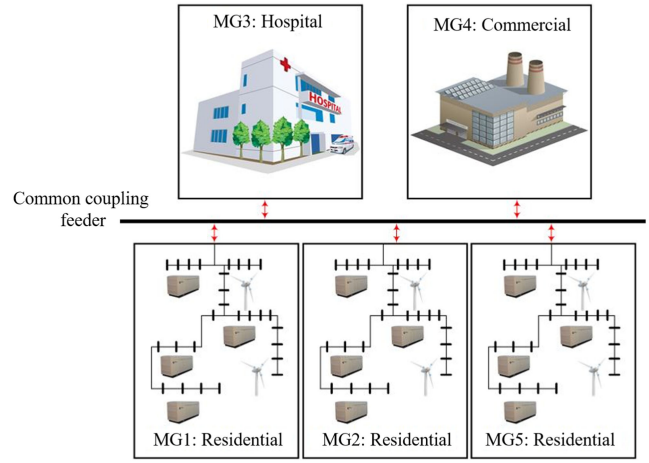

Fig. 1. Interconnected MGs scheme: residential, hospital, and commercial MGs.

A. Objective Function

The objective function (1) minimizes the overall operation cost of the interconnected MGs and consists of four different parts: 1) generation cost of the DGs within each MG; 2) startup and shutdown of DGs; 3) purchasing energy by each MG; 4) selling energy by each MG for a time horizon of 24-hour

$$min \sum_{i,m,t} [(C_{im} P_{imt}) + (S^U_{im} \delta_{imt} + S^D_{im} \delta_{imt}) + (\lambda^P_m P^P_{mt} \delta^P_{mt}) - (\lambda^S_m P^S_{mt})] \quad (1)$$

where $t \in \Omega^T$, $i \in \Omega^{DG}$, and $m \in \Omega^{MG}$ throughout this article. It should be noted that in (1), the output power of DGs, purchasing power, selling power, and status of DGs are decision variables. Also, for the cost of DGs in (1), only controllable DGs in the network are considered, e.g., diesel units.

B. Constraints

1) Power Balance Constraint: This constraint guarantees the hourly power balance as indicated as follows:

$$P^P_{mt} - P^S_{mt} + \sum_i P_{imt} + \sum_e P^{ES}_{emt} = \sum_d D_{dmt} \quad \forall m \in \Omega^{MG}\ \forall t \in \Omega^T. \tag{2}$$

2) Purchasing and Selling Power Limitation: The purchasing and selling power of each MG is limited by a minimum and maximum capacity, as follows:

$$\underline{P^P_m}\delta^P_{mt} \le P^P_{mt} \le \overline{P^P_m}\delta^P_{mt}\ \forall m \in \Omega^{MG} \quad \forall t \in \Omega^T \tag{3}$$

$$\underline{P^S_m}\delta^S_{mt} \le P^S_{mt} \le \overline{P^S_m}\delta^S_{mt}\ \forall m \in \Omega^{MG} \quad \forall t \in \Omega^T. \tag{4}$$

3) Unit Generation Capacity: Equation (5) represents the minimum and maximum capacity of each dispatchable unit

$$\underline{P_{im}}\delta imt \le P_{imt}\overline{P_{im}}\delta imt\ \forall m \in \Omega^{MG}\ \forall t \in \Omega^T \tag{5}$$

$$\underline{Q_{im}}\delta imt \le Q_{imt}\overline{Q_{im}}\delta imt\ \forall m \in \Omega^{MG}\ \forall t \in \Omega^T. \tag{6}$$

4) Ramp Up and Ramp Down Constraints: Limits of ramp up/down rate for increasing or decreasing the units' production are represented as follows:

$$P_{imt} - P_{im(t-1)} \le R^U_{im} \quad \forall i \in \Omega^{DG}\ \forall m \in \Omega^{MG} \quad \forall t \in \Omega^T \tag{7}$$

$$P_{im(t-1)} - P_{imt} \le R^D_{im} \quad \forall i \in \Omega^{DG}\ \forall m \in \Omega^{MG} \quad \forall t \in \Omega^T. \tag{8}$$

5) Minimum Up and Downtime Constraints: When a generation unit is turned ON (OFF), it should be run (OFF) for some time before it is turned OFF (ON) again. Accordingly, the following stand for the minimum up and downtime for each generator:

$$\chi^{on}_{im} \ge \tau^U_{im}(\delta_{imt} - \delta_{im(t-1)}) \quad \forall i \in \Omega^{DG}\ \forall m \in \Omega^{MG}\ \forall t \in \Omega^T \tag{9}$$

$$\chi^{off}_{im} \ge \tau^D_{im}(\delta_{im(t-1)} - \delta_{imt}) \quad \forall i \in \Omega^{DG}\ \forall m \in \Omega^{MG}\ \forall t \in \Omega^T. \tag{10}$$

6) Energy Storage Limitations: Each storage unit has a minimum and maximum limitation on charging and discharging rate, as expressed in (10) and (11), respectively. Moreover, the storage unit cannot be in charging and discharging modes simultaneously, as expressed by (12). The state of charge (SOC) is considered by the amount of charged/discharged power in (13) and is also limited by the capacity constraint (14). In addition, energy storage follows a minimum charging and discharging time, as given in (15) and (16), respectively

$$P^{ES}_{emt} \le \overline{P^d_{emt}}\rho_{emt} - \underline{P^c_{emt}}\vartheta_{emt} \quad \forall e \in \Omega^{ES}\ \forall m \in \Omega^{MG}\ \forall t \in \Omega^T \tag{11}$$

$$P^{ES}_{emt} \ge \underline{P^d_{emt}}\rho_{emt} - \overline{P^c_{emt}}\vartheta_{emt} \quad \forall e \in \Omega^{ES}\ \forall m \in \Omega^{MG}\ \forall t \in \Omega^T \tag{12}$$

$$\rho_{emt} + \vartheta_{emt} \le 1; \forall e \in \Omega^{ES}\ \forall m \in \Omega^{MG}\ \forall t \in \Omega^T \tag{13}$$

$$\psi_{emt} = \psi_{em(t-1)} - P_{emt} \quad \forall e \in \Omega^{ES}\ \forall m \in \Omega^{MG}\ \forall t \in \Omega^T \tag{14}$$

$$0 \le \psi_{emt} \le \overline{\psi_{em(t)}}; \forall e \in \Omega^{ES}\ \forall m \in \Omega^{MG}\ \forall t \in \Omega^T \tag{15}$$

$$\chi^c_{em} \ge \tau^c_{emt}(\rho_{emt} - \rho_{em(t-1)}) \quad \forall e \in \Omega^{ES}\ \forall m \in \Omega^{MG}\ \forall t \in \Omega^T \tag{16}$$

$$\chi^d_{em} \ge \tau^d_{emt}(\vartheta_{emt} - \vartheta_{em(t-1)}) \quad \forall e \in \Omega^{ES}\ \forall m \in \Omega^{MG}\ \forall t \in \Omega^T. \tag{17}$$

7) Power Flow Constraints: Equations (18)–(24) represent the ac power flow model in a radial distribution network based on a set of recursive equations called DistFlow branch equations. In this regard, (18) and (19) assure the active and reactive power balances at network buses, respectively; (20) and (21) guarantee the Kirchhoff's voltage law to the distribution and tie lines, respectively. Therefore, the terms $P^L_{ln,t}$ and $Q^L_{ln,t}$ show the active and reactive power flow in the lines, respectively. Also $\Delta V_{nm,t}$ denotes the auxiliary variable, which is zero if line mn is switched on at time period t, and a positive or negative value depending on the difference between the voltages of the sending and receiving ends of line mn. Also, voltages of each node, as well as the current of distribution lines should be within their limits, as expressed in (22)–(24)

$$\sum_{ln\in\Omega^D L}\left[P^L_{ln,t} - R_{ln}(I^L_{ln,t})^2\right] - \sum_{nz\in\Omega^D L} P^L_{nz,t} + P_{imt} + P^P_{mt} - P^S_{mt} + P^{dc}_{emt} - P^c_{emt} = P^d_{mt} \quad \forall i \in \Omega^{DG}\ \forall m \in \Omega^{MG}\ \forall t \in \Omega^T, \forall e \in \Omega^{ES}, \forall d \in \Omega^D \tag{18}$$

$$\sum_{ln\in\Omega^D L}\left[Q^L_{ln,t} - X_{ln}(I^L_{ln,t})^2\right] - \sum_{nz\in\Omega^D L} Q^L_{nz,t} + Q_{imt} = Q^d_{mt} \quad \forall i \in \Omega^{DG}\ \forall m \in \Omega^{MG}\ \forall t \in \Omega^T\ \forall d \in \Omega^D \tag{19}$$

$$(V_{l,t})^2 - (V_{l,t})^2 = 2(R_{ln}P^L_{ln,t} + X_{ln}Q^L_{ln,t}) - (Z_{ln})^2(I^L_{ln})^2 + \Omega V_{ln,t} \quad \forall l, n \in \Omega^B\ \forall ln \in \Omega^{DL}\ \forall t \in \Omega^T \tag{20}$$

$$(V_{n,t})^2(I_{ln,t})^2 = (P^L_{ln,t})^2 + (Q^L_{ln,t})^2 \forall ln \in \Omega^{DL}\ \forall t \in \Omega^T \tag{21}$$

$$\underline{V} \le V_{n,t} \le \overline{V} \forall n \in \Omega^B\ \forall t \in \Omega^T \tag{22}$$

$$|\Delta V_{ln,t}| \le (\overline{V} - \underline{V})(1 - w^L_{ln,t}) \forall ln \in \Omega^{DL}\ \forall t \in \Omega^T \tag{23}$$

$$0 \le I^L_{ln,t} \le \overline{I^L} w^L_{ln,t} \forall ln \in \Omega^{DL}\ \forall t \in \Omega^T. \tag{24}$$

It is worth noting that each MG (agent) performs its optimization separately; that means the proposed problem is a decentralized optimization problem, along with a broadcast ledger

technology and smart contract, where all MGs (agents) solve their own optimization problems. To this end, the blockchain technology is adopted to assure transparency and security of the power trading within the entire network. Also, it is worth noting that the output power of DGs, charging and discharging of energy storage, and binary variables (status of DGs, energy storage, purchasing power, and selling power) are decision variables of the optimization problem.

III. Stochastic Framework Based on UT

The stochastic nature of the MGs imposes uncertainties in the optimization problem, such as hourly load demand and output powers of nondispatchable DGs [such as wind turbines (WTs)]. It is worth noting that in order to model uncertainties, three approaches can be used.

1) Monte Carlo Simulations: This method requires a large number of runs to converge and also it is unable to model the correlated uncertainties.

2) Analytical methods: A simplification or linearization is crucial for these methods.

3) Estimation methods: They have high convergence speeds and also the capability to model the correlated environment [22], [23]. UT is one of the well-known estimation methods. In the UT method, the nonlinear function is considered as a black box. Hence, no simplification or linearization is crucial [24]. Below is a brief description on the UT method.

For a stochastic nonlinear problem $y = f(x)$, y is the uncertain output vector, x is the random input vector, f is the nonlinear function, and the problem has q uncertain parameters. Hence, x is a vector of a length q, with a mean value μ and covariance σ_x. The symmetrical elements of the matrix σ_x are the variance of the uncertain variables. Moreover, the nonsymmetrical elements are the covariance among different uncertain parameters. Therefore, based on the UT method, the mean and covariance output variable of Y (μ_y and σ_y) can be calculated as follows [26].

Step 1: Utilize (25) and (26) to find out $2q + 1$ samples from the input uncertain data

$$x_0 = \mu \tag{25}$$

$$x_\omega = \mu \pm \left(\sqrt{\frac{q}{1 - W^0}\sigma_x}\right)_\omega ; \omega = 1, 2, \ldots, q. \tag{26}$$

In (26), $(\sqrt{q/1 - W^0\sigma_x})$ is the ωth row or column of matrix square root of $(q/1 - W^0\sigma_x)$. Here, W^0 is the weight of the mean valueμ [24].

Step 2: Use (27) and (28) to calculate the weight associated with each x. It is worth noting that the associated weights should satisfy (29)

$$W_\omega = \frac{1 - W^0}{2q}; \omega = 1, 2, \ldots, q \tag{27}$$

$$W_{\omega+q} = \frac{1 - W^0}{2q}; \omega = q + 1, q + 2, \ldots, 2q \tag{28}$$

$$\sum_{\omega=0}^{2q} W_\omega = 1. \tag{29}$$

Step 3: Give $2q + 1$ sample points to the nonlinear function to obtain the output samples according to (30).

$$y_\omega = f(X_\omega). \tag{30}$$

It should be noted that in the UT method, the nonlinear function is considered as a black box. Hence, no simplification or linearization is required.

Step 4: Calculate the covariance σ_y and the mean μ_y of the output variable Y as follows:

$$\mu_y = \sum_\omega W_\omega Y_\omega \tag{31}$$

$$\sigma_y = \sum_\omega W_\omega (Y_\omega - \mu_y)(Y_\omega - \mu_y)^T. \tag{32}$$

IV. Blockchain and Incentive Contracts for Interconnected MGs

This section describes the proposed blockchain-based transaction mechanism. A transaction in the interconnected MGs involves a blochchain model and an incentive contract model, as described in the following sections, followed by a generic example to clarify the procedure.

A. Blockchain Model

Recently, blockchain has attracted a considerable amount of attention in the literature [27]. A blockchain is a developing list of records, called blocks, which are connected using the hash address (HA). Blockchain is adopted in this article to provide a decentralized incentive contract strategy to improve the procedure's security and transparency. To this end, each block, that stands for a trade in the interconnected MGs, possesses a growing HA. When a trade occurs within the network, a new block with a new HA is generated and chained to the previous block by using the previous block's HA. This successive procedure is continued until the last trade takes place.

Blockchain, in general, secures transactions against manipulation and unauthorized access. While the HA cannot be retrieved from the uncommitted members of the network, it is visible by all the active MGs which have participated in the trade. In other words, every member can observe the information of all blocks, assuring transparency within the network. Moreover, there is no need for a central agent to store and access private information and control the transactions among the members, promising a genuinely decentralized approach. Another advantage of blockchain is the smart contract that will be generated, signed, and executed for all users before they join the network.

B. Incentive Contract and Priority Models

Generally, there are two types of markets in the normal operation: 1) the buyer's market; and 2) the seller's market. According to economics, increasing the demand with a constant supply will increase the consumers' costs [28]. In order to provide a competitive market for all players, an incentive contract pricing mechanism is proposed to provide the electricity buyers with different offers based on the amount of the needed power. In this environment, the sellers have an option to offer the prices

according to the demand, considering the power they can provide. To this end, a higher load demand motivates the seller to offer a lower generation price to win in the tender, providing an option for each MG to reduce their costs during a one-time transaction.

A priority system delivers the power to each MG based on the importance level of the load. This system ranks the MGs according to the nature of their load, and a higher priority is granted to critical loads, such as hospital and public services. The loads of medium importance are considered as commercial loads, and the lowest priority is assigned to residential loads.

C. Numerical Example

This section clarifies the above concepts through a generic example. Considering that MG1 (residential load) and MG3 (hospital) are short in the next hour, of $P = 250$ kW and $P = 100$ kW, respectively. These demands are announced by generating a new block with the associated HA of $X1$, showing to the committed MGs that $P = 350$ kW is needed at the next hour. Once the request is submitted on the ledger, other participants offer their prices based on their own capability to provide the power. For example, MG2 is able to provide a maximum power of $P = 300$ kW at the price of 4.5\$/kWh, and its offers are as follows: (*i*) 4.50 \$/kWh for purchases $P \leq 30$ kW, (*ii*) 4.0 \$/kWh for purchases $30\,\text{kW} \leq P \leq 60$ kW, and (*iii*) 3.80 \$/kWh for purchases $P \geq 60$ kW. Furthermore, MG5 is able to provide a maximum power of $P = 200$ kW at the price of 3.70\$/kWh if the buyer purchases all the power.

According to the priority list, the blockchain first introduces all the offers to MG3 (the load with the highest priority), and MG3 has to decide to accept the offers within 1 minute. If MG3 accepts these offers in time, the blockchain subtracts the MG3's demand from the offers and introduces the modified offers to MG1. If MG3 does not accept the offers in the given time, the blockchain will introduce all the offers to the next demand in the priority list (MG1). It should be noted that in the blockchain technology, different with the traditional mining process, a smart contract and priority list will be determined for power transactions within the network. For example, the hospital as the first priority MG may be the first user to complete the transaction, even if a commercial MG can provide a better deal. In this priority system, no computation burden is put on the MG user side, but the presetting priority level is used. Also, unlike the conventional approach, in the blockchain technology, the smart contract and priority list will determine power transactions within the network; that means no centralized agency is required to control the price or portfolio. Moreover, the system is transparent for all active members to mitigate financial fraud and reduce system risks. It is worth noting that the users share their information/marketing data based on their privacy concerns or judgment. The data provided by them is either publicly available information or safe to be put in public. All participants can make their own decisions based on the public data broadcasted by others.

V. Solution Procedure

In this section, the solution procedure of the proposed problem is explained in detailed steps as follows.

Step 1: Define the following parameters: the number of MGs, number of generators for each MG, generator characteristics, energy storage characteristics, incentive contract price charts, priority of each MG, number of uncertain parameters, and parameter settings for the optimization problem.

Step 2: Use (25)–(32) to model the uncertainty in WTs output and load demand.

Step 3: Solve the optimization problem for each MG. Then, calculate the maximum generation power for each DG within each MG.

If the maximum generation power is more than the load demand within the MG, then

1) calculate the extra power;
2) solve the optimization problem (1)–(16);
3) go to Step 9.

Else Go to Step 4.

Step 4: Calculate the extra power for each generator to be shared with other areas.

Step 5: Evaluate the generation strategy (constraints) for each area and the power mismatch by blockchain.

Step 6: Utilize blockchain to solve the optimal dispatch with the minimal cost of purchase strategy based on the pricing strategy (buy-now price) described in Table III

Step 7: Check the priority of the MG(s) that need(s) a transaction and add the highest priority block to the trade chain. Use Table III to make a price change (buy-later price) for lower priority MG(s) on generators in Step 6.

Step 8: Update the blockchain ledger and check if all MGs power is balanced, otherwise go to Step 6.

Step 9: Evaluate the expected value of the cost objective function based on (1), by utilizing the incentive contract chart and UT output.

Step 10: if the result is feasible, *then* finish the algorithm and calculate the total cost,

else Go to Step 3.

The blockchain-based decentralized energy management procedure is depicted in Fig. 2. It should be noted that the system is simulated based on an hourly interval; that means the data will be transferred to the main storage (usually a cloud) in each hour.

VI. Simulation Results

A. Data Summary

In order to demonstrate the effectiveness of the proposed method, five interconnected MGs are selected, as shown in Fig. 1. The system contains three residential MGs (MG1, MG2, MG5), one hospital MG (MG3), and one commercial MG (MG4). Fig. 3 shows the 24-hours load duration curves for each MG, obtained from a real test system in Baton Rouge, LA, USA [29]. Tables I and II show the characteristics of DGs and energy storage within each MG, respectively. Moreover, each MG includes two wind turbines (WTs) that are correlated with

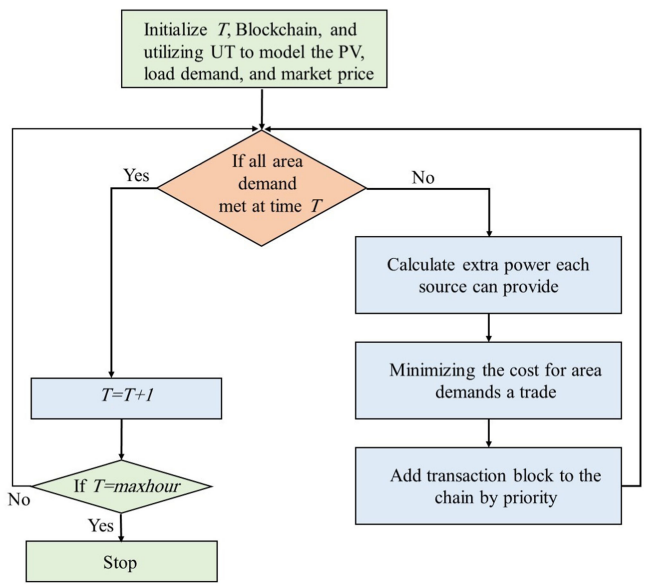

Fig. 2. Flowchart of decentralized energy management based on the blockchain for each area.

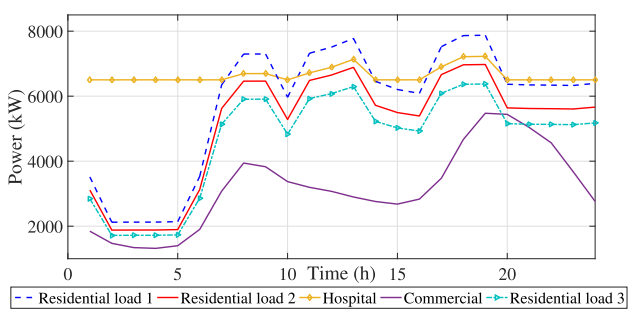

Fig. 3. 24-hour load demand within each MG.

TABLE I
CHARACTERISTICS OF DGS IN EACH MG

MG No.	Priority Level	C_{im} (\$/kWh)	DG Unit	$\underline{P_{im}}/\overline{P_{im}}$ (kW)	τ^U_{im}/τ^D_{im} (h)
MG1	3	2.3	DG1	400/1500	2/2
		2.5	DG2	500/2500	3/3
		2.6	DG3	600/2000	3/3
		3.1	DG4	500/2000	1/1
MG2	3	2.1	DG1	600/1500	3/3
		2.5	DG2	700/1800	3/3
		2.7	DG3	400/1500	2/2
		2.9	DG4	400/1500	2/2
MG3	1	2.1	DG1	500/2500	3/3
		2.2	DG2	600/2000	3/3
		2.5	DG3	400/3000	2/2
		2.6	DG4	400/2000	1/1
MG4	2	2.3	DG1	800/1500	3/3
		2.5	DG2	400/1800	2/2
		2.6	DG3	800/2000	2/2
MG5	3	2.3	DG1	800/3000	2/2
		2.4	DG2	700/2500	1/1
		2.6	DG3	400/2500	3/3
		2.8	DG4	800/1800	4/4

TABLE II
CHARACTERISTICS OF ENERGY STORAGE SYSTEMS (ESS)

Capacity (kWh)	Min-Max of Charging/Discharging Power (kW)	Min-Max of Charging/Discharging Time (h)
800	0-200	5

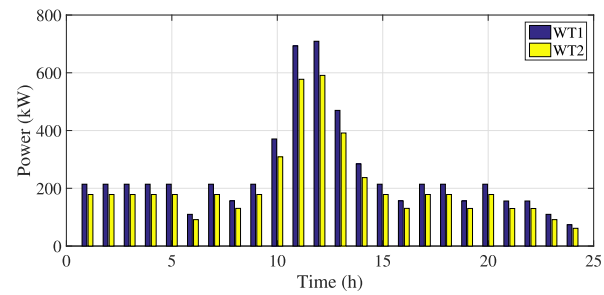

Fig. 4. Wind turbines output power in each area.

TABLE III
INCENTIVE CONTRACT PRICE OF INTERCONNECTED MGS

Power Offer	Buy-Now Price	Buy-Later Price
Less than 10%	Listing Price	10% more of buy-now price
10%-20%	5% off of listing price	10% more of buy-now price
More than 20%	10% off of listing price	10% more of buy-now price

each other (and the correlation coefficient is 1.3) and have the same patterns, as shown in Fig. 4.

The incentive contract pricing associated with the problem is defined based on Table III. For instance, if the power to be purchased is less than 10% of the DG capacity, the price would be the same as the listing price shown in Table I. If the power to be purchased is between $10\% - 20\%$ of the capacity of DG, the price is reduced to 95% of the listing price (that means 5% less than the listing price). Finally, if the power to be purchased is more than 20% of the capacity of DG, then the price is 90% of the listing price. Such an incentive contract pricing mechanism motivates the load consumers to increase their purchase power when being beneficial from the lower price per power unit. Also, it should be noted that the buy-now price denotes the price for the first buyer at time t. Consequently, the buy-later price refers to the second buyer at time t. The incentive contract can be considered as a package of common rules, restrictions, and boundaries that every member agrees and will be automatically executed. In this study, an incentive contract is designed based on the restrictions on the power generation, power sources limitations, pricing, and priority agreement. It is worth noting that the selling price is 50% more than the generation cost in Table I, i.e., the DGs prices will be increased by 50% if in the selling mode.

B. Case Study Results

Figs. 5–9 show the active power (i.e., real power) of the generation units. It is seen that the cheapest DGs are committed more

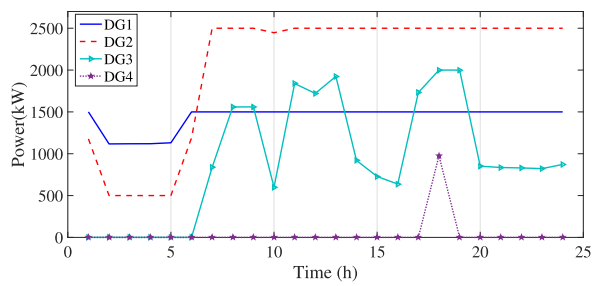

Fig. 5. Active power output of MG1.

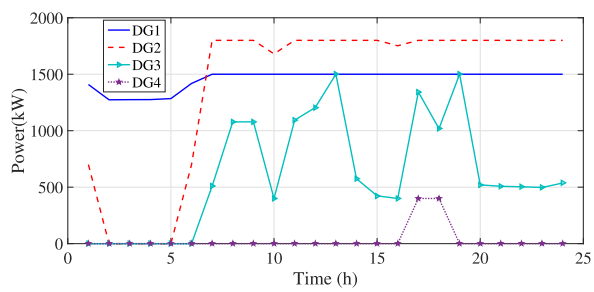

Fig. 6. Active power output of MG2.

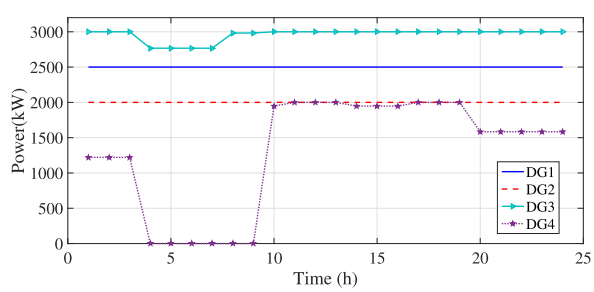

Fig. 7. Active power output of MG3.

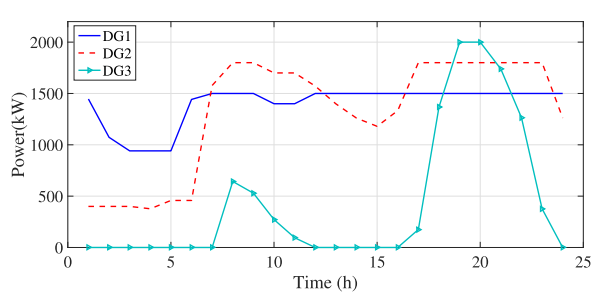

Fig. 8. Active power output of MG4.

frequently than others. For instance, in the first MG (see Fig. 5), DG 1 and DG 2 are operated with the maximum capacities during the study period, indicating the efficient performance of the algorithm. According to the simulation results, units are committed only based on the economic consideration. According to Figs. 5–9, the cheapest DG (i.e., DG1) is more committed than others in each MG. Accordingly, the most expensive one (i.e., the last DG) in each MG is less committed than others.

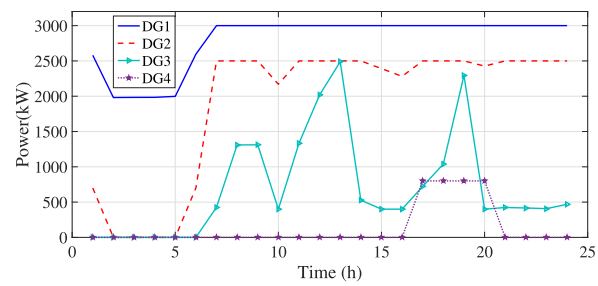

Fig. 9. Active power output of MG5.

Table IV presents an instance of the real-time blockchain energy management agenda for all MGs, which is updated at the end of each iteration for each MG. For example, at hour 11, MG3 (Area 3) receives an amount of power of 232.977 kW from MG1 (Area 1). This energy is provided by the third DG (Gen3) in MG1 (see index 1 in Table IV). In another transaction at hour 12, MG3 receives an amount of power of 456.210 kW from DG3 (Gen3) in MG5. As shown in Figs. 6 and 7, at hours 11 and 12, all the units within MG3 are committed at their maximum capacities. Since its load demand exceeds the maximum power of all DGs within the area, MG3 has to purchase energy from another MG. At hour 19, MG3's demand cannot be satisfied by one area only. Hence, MG3 receives 406.7813 kW power from MG2 and 125 kW power from MG5, provided by the DGs 1 and 2, respectively. It should be noted that based on the results in Table IV, MG3 (hospital) and MG4 (commercial MG), as the first and second priority load, respectively, receive most of the energy. Also, each MG tries to purchase energy from the cheapest units of other MGs. For instance, at hour 20, MG 4 receives more than 65% of its extra demand from the cheapest DG in MG1 (DG1). In another example, at hour 13, MG3 receives more than 90% of its extra demand from the cheapest generator of MG2 (DG1) (see Table IV). It should be noted that sellers are responsible for the cost of power losses. Hence, the net power will be delivered to the requested area. It is also assumed that all the generated renewable power (e.g., wind and solar) will be consumed and the remained amount of load demand (i.e., net load) will be covered by other generation units. Thus, excessive wind/solar power won't be challenging if the wind/solar penetration level is low. However, the spinning reserve (that is 2% of the load demand at any hour) is considered in the case of power shortage of renewable generators or unit outages.

Also, Table IV shows the HA addresses of each transaction. Based on the table, each transaction (block) contains two HA including both previous hash and self-hash, which are changing for each transaction (block). Therefore, each block will be added to the previous one based on the previous HA, which generates a new HA that can lead to higher security within the system. For instance, the previous HA of the block at hour 12 is the same as the self-hash address of hour 11. Also, this block is generating a new HA that is accessible by all active members.

Fig. 10 presents the energy storage's SOC within each MG. As shown in the figure, the SOC levels for different energy storage

TABLE IV
BLOCKCHAIN-BASED ENERGY MANAGEMENT

index:	0
time:	-1
data:	'Genesis Block'
previous Hash:	[]
self-Hash:	'244c2f2c45e14b150bc35767a903048cd2895d0202 3a63d344eba2b261dbdfbd'
priority:	[]
index:	1
time:	11
data:	'Area 3' 'Area 1' 'Gen 3' '232.9778' 'KW'
previous Hash:	'244c2f2c45e14b150bc35767a903048cd2895d0202 3a63d344eba2b261dbdfbd'
self-Hash:	'0b8adf789b6f273bef8025729183d00d'
priority:	1
index:	2
time:	12
data:	'Area 3' 'Area 5' 'Gen 3' '456.2101' 'KW'
previous Hash:	'0b8adf789b6f273bef8025729183d00d'
self-Hash:	'99a37e4eaf9caad5841bb8d3b433e77d'
priority:	1
index:	3
time:	13
data:	'Area 3' 'Area 1' 'Gen 3' '61.9142' 'KW' 'Area 3' 'Area 2' 'Gen 1' '712.9401' 'KW'
previous Hash:	'99a37e4eaf9caad5841bb8d3b433e77d'
self-Hash:	'71c5891d4457efac4d15209c65be7bde'
priority:	1
index:	4
time:	17
data:	'Area 3' 'Area 5' 'Gen 3' '473.2676' 'KW'
previous Hash:	'71c5891d4457efac4d15209c65be7bde'
self-Hash:	'2dcaa2cffef1c5ee8356b12fa16e5ab4'
priority:	1
index:	5
time:	18
data:	'Area 3' 'Area 1' 'Gen 1' '880.389' 'KW'
previous Hash:	'2dcaa2cffef1c5ee8356b12fa16e5ab4'
self-Hash:	'bc7792574e46a582a1e8972d2ab5761c'
priority:	1
index:	6
time:	19
data:	'Area 3' 'Area 2' 'Gen 1' '406.7813' 'KW' 'Area 3' 'Area 5' 'Gen 2' '125' 'KW'
previous Hash:	'bc7792574e46a582a1e8972d2ab5761c'
self-Hash:	'8dc355c25ff054c4a8db4845fcbfec18'
priority:	1
index:	7
time:	19
data:	'Area 4' 'Area 2' 'Gen 2' '913.4125' 'KW'
previous Hash:	'8dc355c25ff054c4a8db4845fcbfec18'
self-Hash:	'99127e26ba7632814bd1d0e3b0f3d465'
priority:	2
index:	8
time:	20
data:	'Area 4' 'Area 1' 'Gen 1' '567.9741' 'KW' 'Area 4' 'Area 1' 'Gen 4' '132.6789' 'KW' 'Area 4' 'Area 2' 'Gen 4' '160.3727' 'KW'
previous Hash:	'99127e26ba7632814bd1d0e3b0f3d465'
self-Hash:	'641c14f862af701c76268f1badcb9850'
priority:	2
index:	9
time:	20
data:	'Area 4' 'Area 1' 'Gen 3' '104.1741' 'KW' 'Area 4' 'Area 1' 'Gen 4' '153.4476' 'KW'
previous Hash:	'641c14f862af701c76268f1badcb9850'
self-Hash:	'797e01ef6f46e86c329a13f39f2a1a6e'
priority:	2

systems have followed a similar pattern as the load demands (see Figs. 3 and 10). Based on the figure, the energy storage is committed more in critical areas like the hospital MG.

Fig. 11 compares the total operating cost by using deterministic and stochastic models under different scenarios. While considering the uncertainties has resulted in incremental costs

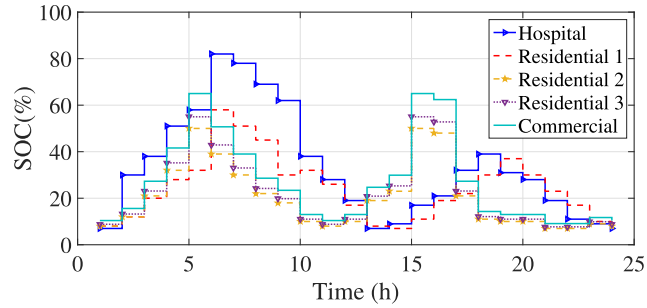

Fig. 10. Battery storage system SOC in each MG.

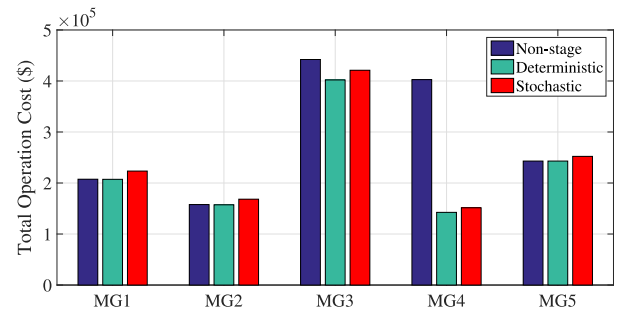

Fig. 11. Comparison of operation cost under stochastic and deterministic conditions.

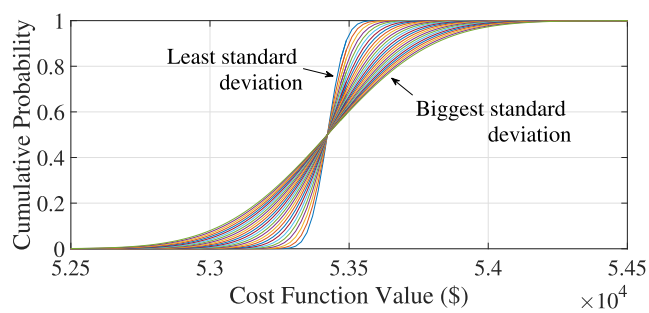

Fig. 12. Impact of standard deviation of the random variables on the cost function.

in all scenarios, the solution will be more reliable since the uncertainties in WTs power and load demand forecasts are characterized, as shown in Fig. 12. Fig. 12 shows the cumulative distribution of the cost objective function with different standard deviation values. It is observed that increasing the standard deviation value of the random variables can potentially cause higher risks in the cost objective function.

Table V presents the total operation cost for both centralized (without blockchain) and decentralized (considering blockchain) approaches. According to this table, the operation cost of the centralized conventional approach is more than that of the decentralized blockchain approach. This is mainly because in the conventional approach, the network should pay extra money to the central point (e.g., DSO) for effective power dispatching within the network. Table V also compares the total network

TABLE V
TOTAL OPERATION COST FOR BOTH CENTRALIZED (WITHOUT BLOCKCHAIN) AND DECENTRALIZED (WITH BLOCKCHAIN) APPROACHES

Technique	Centralized Method ($)	Decentralized Method ($)
Proposed Technique	1,251,756	1,152,100
Stochastic programming [30]	1,276,237	1,167,054
Robust optimization [31]	1,283,692	1,190,119

operation costs with both centralized and decentralized approaches, using MILP, stochastic programming [30], and robust optimization [31] techniques. It is observed from Table V that the proposed technique has a lower operation cost, compared to the robust optimization and stochastic programming techniques. Please note that the total operation cost of the proposed technique in Table V includes the cost of using the blockchain technology. However, the cloud storage cost is neglected since it is the same for both the conventional and proposed approaches.

C. Discussion

This article investigates the optimal energy management of interconnected MGs based on the blockchain technique. As shown in the simulation results, the following features are identified.

1) *Security:* One of the significant achievements of the proposed blockchain-based model is security improvement within the networked MG. Utilizing the blockchain can lead to an unbreakable chain, while every hash containing the previous information, can contribute to higher security.
2) *Transparency:* One of the benefits of the blockchain theory is transparency of transactions within the network. Indeed, every block is generated and added to the chain, while broadcasting to all members who join the blockchain. Moreover, all MGs are able to see the information transferring among all the blocks, which can lead to transparency within the network.
3) *Decentralization:* Furthermore, there is no need to have a centralized agent to keep private information and control the transactions among members. This can bring two benefits: a) Less operational cost: Usually, the central agent incurs costs, since all members have to compensate extra the central agent for each transaction. b) Prevent financial corruption: Access to all chain blocks can potentially lead to safe transactions and avoid financial corruption. Indeed, each member of the chain, must have a transparent transaction that will be added as a new block to the last block in the chain.
4) *Cost reduction:* The last but not least benefit of utilizing the blockchain technology is minimizing the operation cost of the entire network. Based on Table V, the operation cost of the proposed method is less than that of the conventional centralized method. This lower cost (i.e., 8%) is attributed to effective energy management within the network as well as the preventive cost to the central node.

VII. CONCLUSION

This article developed a secure, transparent, and decentralized blockchain technique for optimal scheduling of interconnected MGs. Employing the blockchain technology can lead to system security improvement as well as lower system risks, mitigate financial fraud, and cut down the operational cost. A stochastic framework according to the UT method was developed to model the uncertainties in hourly load demand and renewable energy output. Moreover, an incentive contract price was developed to increase the purchasing power and reduce the selling price. In addition, a priority list was developed for all types of MGs, and based on the list, critical loads such as hospital and commercial MGs should be satisfied first. According to the simulation results, utilizing the decentralized blockchain method has brought lower operational cost and transparency of energy management within the network. Furthermore, due to the changing address in each iteration and the removal of central node, the security of the system could also be enhanced. Potential future work will explore the real-time monitoring of the system in the present of generation unit's outage or cyber/physical attacks.

REFERENCES

[1] Z. Wang, B. Chen, J. Wang, M. M. Begovic, and C. Chen, "Coordinated energy management of networked microgrids in distribution systems," *IEEE Trans. Smart Grid*, vol. 6, no. 1, pp. 45–53, Jan. 2015.
[2] M. Dabbaghjamanesh, A. Kavousi-Fard, and Z. Y. Dong, "A novel distributed cloud-fog based framework for energy management of networked microgrids," *IEEE Trans. Power Syst.*, vol. 35, no. 4, pp. 2847–2862, Jul. 2020.
[3] M. Dabbaghjamanesh, S. Mehraeen, A. Kavousi-Fard, and F. Ferdowsi, "A new efficient stochastic energy management technique for interconnected AC microgrids," in *Proc. IEEE Power Energy Soc. Gen. Meeting*, 2018, pp. 1–5.
[4] Z. Wang, B. Chen, J. Wang, J. Kim, and M. M. Begovic, "Robust optimization based optimal DG placement in microgrids," *IEEE Trans. Smart Grid*, vol. 5, no. 5, pp. 2173–2182, Sep. 2014.
[5] A. Khodaei, "Microgrid optimal scheduling with multi-period islanding constraints," *IEEE Trans. Power Syst.*, vol. 29, no. 3, pp. 1383–1392, May 2014.
[6] S. Wencong, and J. Wang, "Energy management systems in microgrid operations," *Electricity J.*, 25, no. 8, pp. 45–60, 2012.
[7] W. Su, J. Wang, and J. Roh, "Stochastic energy scheduling in microgrids with intermittent renewable energy resources," *IEEE Trans. Smart Grid*, vol. 5, no. 4, pp. 1876–1883, Jul. 2014.
[8] Y. Liu, C. Yuen, N. Ul Hassan, S. Huang, R. Yu, and S. Xie, "Electricity cost minimization for a microgrid with distributed energy resource under different information availability," *IEEE Trans. Ind. Electron.*, vol. 62, no. 4, pp. 2571–2583, Apr. 2015.
[9] S. Parhizi, A. Khodaei, and M. Shahidehpour, "Market-based versus price-based microgrid optimal scheduling," *IEEE Trans. Smart Grid*, vol. 9, no. 2, pp. 615–623, Mar. 2018.
[10] C. Zhang, Y. Xu, Z. Y. Dong, and J. Ma, "Robust operation of microgrids via two-stage coordinated energy storage and direct load control," *IEEE Trans. Power Syst.*, vol. 32, no. 4, pp. 2858–2868, Jul. 2017.
[11] H. S. V. S. Kumar Nunna and S. Doolla, "Multiagent-based distributed-energy-resource management for intelligent microgrids," *IEEE Trans. Ind. Electron.*, vol. 60, no. 4, pp. 1678–1687, Apr. 2013.
[12] M. Dabbaghjamanesh, A. Kavousi-Fard, and S. Mehraeen, "Effective scheduling of reconfigurable microgrids with dynamic thermal line rating," *IEEE Trans. Ind. Electron.*, vol. 66, no. 2, pp. 1552–1564, Feb. 2019.
[13] H. S. V. S. K. Nunna and S. Doolla, "Demand response in smart distribution system with multiple microgrids," *IEEE Trans. Smart Grid*, vol. 3, no. 4, pp. 1641–1649, Dec. 2012.
[14] M. Fathi and H. Bevrani, "Adaptive energy consumption scheduling for connected microgrids under demand uncertainty," *IEEE Trans. Power Del.*, vol. 28, no. 3, pp. 1576–1583, Jul. 2013.

[15] G. E. Asimakopoulou, A. L. Dimeas, and N. D. Hatziargyriou, "Leader-follower strategies for energy management of multi-microgrids," *IEEE Trans. Smart Grid*, vol. 4, no. 4, pp. 1909–1916, Dec. 2013.
[16] N. Nikmehr and S. Najafi Ravadanegh, "Optimal power dispatch of multi-microgrids at future smart distribution grids," *IEEE Trans. Smart Grid*, vol. 6, no. 4, pp. 1648–1657, Jul. 2015.
[17] Y. Zhang, N. Gatsis, and G. B. Giannakis, "Robust energy management for microgrids with high-penetration renewables," *IEEE Trans. Sustain. Energy*, vol. 4, no. 4, pp. 944–953, Oct. 2013.
[18] Z. Wang, B. Chen, J. Wang, and J. kim, "Decentralized energy management system for networked microgrids in grid-connected and islanded modes," *IEEE Trans. Smart Grid*, vol. 7, no. 2, pp. 1097–1105, Mar. 2016.
[19] S. Wang, L. Ouyang, Y. Yuan, X. Ni, X. Han, and F. Wang, "Blockchain-enabled smart contracts: Architecture, applications, and future trends," *IEEE Trans. Syst., Man, Cybern.: Syst.*, vol. 49, no. 11, pp. 2266–2277, Nov. 2019.
[20] Y. Yuan and F. Wang, "Blockchain and cryptocurrencies: Model, techniques, and applications," *IEEE Trans. Syst., Man, Cybern.: Syst.*, vol. 48, no. 9, pp. 1421–1428, Sep. 2018.
[21] Y. Liu, K. Wang, Y. Lin, and W. Xu, "LightChain: A lightweight blockchain system for industrial internet of things," *IEEE Trans. Ind. Inform.*, vol. 15, no. 6, pp. 3571–3581, Jun. 2019.
[22] J. Wan, J. Li, M. Imran, D. Li, and Fazal-e-Amin, "A blockchain-based solution for enhancing security and privacy in smart factory," *IEEE Trans. Ind. Inform.*, vol. 15, no. 6, pp. 3652–3660, Jun. 2019.
[23] MH M. OboudiMohammadi, and M.Rastegar, "Resilience-oriented intentional islanding of reconfigurable distribution power systems," *J. Modern Power Syst. Clean Energy*, vol. 7, no. 4, pp. 741–752, 2019.
[24] M. Aien, M. Fotuhi-Firuzabad, and F. Aminifar, "Probabilistic load flow in correlated uncertain environment using unscented transformation," *IEEE Trans. Power Syst.*, vol. 27, no. 4, pp. 2233–2241, Nov. 2012.
[25] M. Dabbaghjamanesh, S. Mehraeen, A. Kavousifard, and M. A. Igder, "Effective scheduling operation of coordinated and uncoordinated wind-hydro and pumped-storage in generation units with modified JAYA algorithm," in *Proc. IEEE Ind. Appl. Soc. Annu. Meeting*, 2017, pp. 1–8.
[26] M. Aien, M. Fotuhi-Firuzabad, and F. Aminifar, "Probabilistic load flow in correlated uncertain environment using unscented transformation," *IEEE Trans. Power Systems*, vol. 27, no. 4, pp. 2233–2241, Nov. 2012.
[27] P. Vigna and Mi. J. Casey, *The Age of Cryptocurrency: How Bitcoin and the Blockchain are Challenging the Global Economic Order*. New York, NY, USA: Macmillan, 2016.
[28] M. Pisa and M. Juden, "Blockchain and economic development: Hype vs. reality," *Center Glob. Develop. Policy Paper*, vol. 107, p. 150, 2017.
[29] Comercial Load Data, Aug. 2018. [Online]. Available: https://openei.org/datasets
[30] Y. Zhan, Q. P ZhengJ. Wang, and P.Pinson, "Generation expansion planning with large amounts of wind power via decision-dependent stochastic programming," *IEEE Trans. Power Syst.* vol. 32, no. 4, pp. 3015–3026, Jul. 2017.
[31] G. Liu, Y. Xu, and K. Tomsovic, "Bidding strategy for microgrid in day-ahead market based on hybrid stochastic/robust optimization," *IEEE Trans. Smart Grid*, vol. 7, no. 1, pp. 227–237, Jan. 2016.

Morteza Dabbaghjamanesh (Senior Member, IEEE) received the M.Sc. degree in electrical engineering from Northern Illinois University, DeKalb, IL, USA, in 2014, and the Ph.D. degree in electrical and computer engineering form Louisiana State University, Baton Rouge, LA, USA in 2019.

Currently, he is a Research Associate with the Design and Optimization of Energy Systems (DOES) Laboratory, The University of Texas at Dallas, Richardson, TX, USA. His current research interests include power system operation and planning, reliability, resiliency, renewable energy sources, cybersecurity analysis, machine/deep learning, smart grids, and microgrids.

Boyu Wang (Member, IEEE) received the B.S. degree in electrical engineering from the Harbin Institute of Technology, Weihai, China in 2012, and the M.S. and Ph.D. degrees in electrical and computer engineering from Louisiana State University, Baton Rouge, LA, USA, in 2014 and 2019, respectively.

He currently works as a Senior Data Scientist with Tacoma Public Utilities, Tacoma, WA, USA. His research interests include decentralized optimal control, power system stability analysis, and machine learning in power system.

Abdollah Kavousi-Fard (Senior Member, IEEE) received the B.Sc. degree from the Shiraz University of Technology, Shiraz, Iran, in 2009, the M.Sc. degree from Shiraz University, Shiraz, in 2011, and the Ph.D. degree from the Shiraz University of Technology in 2016, all in electrical engineering.

He is currently an Assistant Professor with the Shiraz University of Technology since 2018. He was a Postdoctoral Research Assistant with the University of Michigan, Ann Arbor, MI, USA, from 2016 to 2018. He was a Researcher with the University of Denver, Denver, CO, USA from 2015 to 2016 conducting research on microgrids. His current research interests include advanced machine learning in power systems, operation, management and cyber security analysis of smart grids, microgrid, smart city, electric vehicles as well as protection of power systems, reliability, and artificial intelligence.

Dr Kavousi-Fard is an Editor in IEEE Transactions on Industrial Applications, in *Springer*, and also in *ISTE ISI Journal*.

Nikos D. Hatziargyriou (Life Fellow, IEEE) is a Professor in power systems with the National Technical University of Athens, Athens, Greece. He has over 10 years industrial experience as the Chairman and CEO of the Hellenic Distribution Network Operator and as the Executive Vice-Chair of the Public Power Corporation. He has participated in more than 60 RD&D projects funded by the EU Commission, electric utilities, and manufacturers for both fundamental research and practical applications. He is author of the book *Microgrids: Architectures and Control*, more than 250 journal publications, and 500 conference proceedings papers.

Dr. Hatziargyriou was the Chair and currently the Vice-chair of the EU Technology and Innovation Platform on Smart Networks for Energy Transition (ETIP-SNET) representing E.DSO. He is the Honorary Member of CIGRE and past Chair of CIGRE SC C6 "Distribution Systems and Distributed Generation". He is the past Chair of the Power System Dynamic Performance Committee (PSDPC) and currently the Editor in Chief of the IEEE Transactions on Power Systems. He is included in the 2016, 2017, and 2019 Thomson Reuters lists of the top 1% most cited researchers.

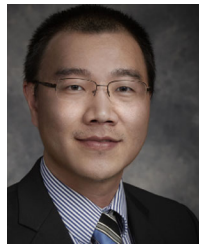

Jie Zhang (Senior Member, IEEE) received the B.S. and M.S. degrees in mechanical engineering from the Huazhong University of Science and Technology, Wuhan, China, in 2006 and 2008, respectively, and the Ph.D. degree in mechanical engineering from Rensselaer Polytechnic Institute, Troy, NY, USA, in 2012.

He is currently an Assistant Professor with the Department of Mechanical Engineering and the Department of Electrical and Computer Engineering (Affiliated), The University of Texas at Dallas, Richardson, TX, USA. His research interests include multidisciplinary design optimization, complex engineered systems, big data analytics, wind and solar forecasting, renewable integration, and energy systems modeling and simulation.